



日本原子力研究開発機構機関リポジトリ  
Japan Atomic Energy Agency Institutional Repository

Title	Rapid measurement scheme for texture in cubic metallic materials using time-of-flight neutron diffraction at iMATERIA
Author(s)	Onuki Yusuke, Hoshikawa Akinori, Sato Shigeo, Xu P. G., Ishigaki Toru, Saito Yoichi, Todoroki Hidekazu, Hayashi Makoto
Citation	Journal of Applied Crystallography,49(5),p.1579-1584
Text Version	Publisher's Version
URL	<a href="https://jopss.jaea.go.jp/search/servlet/search?5055948">https://jopss.jaea.go.jp/search/servlet/search?5055948</a>
DOI	<a href="https://doi.org/10.1107/S160057671601164X">https://doi.org/10.1107/S160057671601164X</a>
Right	©2016 International Union of Crystallography



## Rapid measurement scheme for texture in cubic metallic materials using time-of-flight neutron diffraction at iMATERIA

Yusuke Onuki, Akinori Hoshikawa, Shigeo Sato, Pingguang Xu, Toru Ishigaki, Yoichi Saito, Hidekazu Todoroki and Makoto Hayashi

*J. Appl. Cryst.* (2016). **49**, 1579–1584



**IUCr Journals**  
CRYSTALLOGRAPHY JOURNALS ONLINE

Copyright © International Union of Crystallography

Author(s) of this paper may load this reprint on their own web site or institutional repository provided that this cover page is retained. Republication of this article or its storage in electronic databases other than as specified above is not permitted without prior permission in writing from the IUCr.

For further information see <http://journals.iucr.org/services/authorrights.html>

# Rapid measurement scheme for texture in cubic metallic materials using time-of-flight neutron diffraction at iMATERIA

Yusuke Onuki,<sup>a,\*</sup> Akinori Hoshikawa,<sup>a</sup> Shigeo Sato,<sup>a,b</sup> Pinguang Xu,<sup>c</sup> Toru Ishigaki,<sup>a</sup> Yoichi Saito,<sup>d</sup> Hidekazu Todoroki<sup>d</sup> and Makoto Hayashi<sup>e</sup>

Received 26 April 2016

Accepted 17 July 2016

Edited by Th. Proffen, Oak Ridge National Laboratory, USA

**Keywords:** crystallographic texture; neutron diffraction; Rietveld texture analysis; iMATERIA; steels.

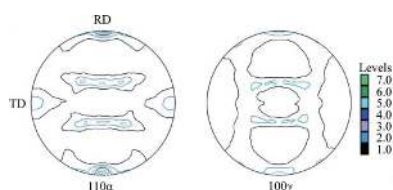
<sup>a</sup>Frontier Research Center for Applied Atomic Sciences, Ibaraki University, 162-1 Shirakata, Tokai, Ibaraki 319-1106, Japan, <sup>b</sup>Graduate School of Science and Engineering, Ibaraki University, 4-12-1 Narusawa-cho, Hitachi, Ibaraki 316-8511, Japan, <sup>c</sup>Japan Atomic Energy Agency, 2-4 Shirakata, Tokai, Ibaraki 319-1106, Japan, <sup>d</sup>Nippon Yakin Kogyo Co. Ltd, 4-2 Kojima-cho, Kawasaki, Kanagawa 210-8558, Japan, and <sup>e</sup>CROSS Tokai, 162-1 Shirakata, Tokai, Ibaraki 319-1106, Japan. \*Correspondence e-mail: yusuke.onuki.0@vc.ibaraki.ac.jp

A rapid texture measurement system has been developed on the time-of-flight neutron diffractometer iMATERIA (beamline BL20, MLF/J-PARC, Japan). Quantitative Rietveld texture analysis with a neutron beam exposure of several minutes without sample rotation was investigated using a duplex stainless steel, and the minimum number of diffraction spectra required for the analysis was determined experimentally. The rapid measurement scheme employs 132 spectra, and by this scheme the quantitative determination of volume fractions of texture components in ferrite and austenite cubic phases in a duplex stainless steel can be made in a short time. This quantitative and rapid measurement scheme is based on the salient features of iMATERIA as a powder diffractometer, *i.e.* a fairly high resolution in  $d$  spacing and numerous detectors covering a wide range of scattering angle.

## 1. Introduction

Crystallographic texture is recognized as an important factor that can control the properties of materials. The recent development and popularization of electron backscatter diffraction (EBSD) measurements have aided in the clarification of local and spatial crystal orientation distributions of materials and related phenomena (Onuki *et al.*, 2013). However, to consider the texture as an overall property of a material, statistically sufficient information from a large enough volume is necessary. Pole figure measurements using X-rays have typically been used for this purpose, along with orientation distribution function (ODF) calculations (Kocks *et al.*, 1998). However, the X-ray beam penetration depths in metallic materials are limited to a few tens of micrometres. Therefore, both X-ray and EBSD measurements can only represent the texture on the measured surface, while many engineering materials have inhomogeneous texture distributions through their thickness. For example, the layer on the surface and the thickness centre of a rolled sheet often have different textures (Truszkowski *et al.*, 1982).

A beam of neutrons has a high transmittance in most metals, so it can be an ideal quantum beam for texture measurements to investigate the overall properties of materials. This advantage of neutron diffraction has been recognized in multiple published studies (Jensen & Kjems, 1983; Oles *et al.*, 1985; Wenk, 1991). Additionally, the recent development of whole-spectrum analysis using time-of-flight (TOF) neutron diffraction has enabled the analysis of textures in multiphase materials (Matthies *et al.*, 1997, 1999; Wenk *et al.*, 2010).



© 2016 International Union of Crystallography

The present authors have developed a neutron-beam texture measurement system based on the Ibaraki Materials Design Diffractometer, iMATERIA, on beamline BL20 at the Material and Life Science Facility of the Japan Proton Accelerator Research Complex (MLF/J-PARC, Japan). In addition to the above-mentioned advantages of TOF neutron diffraction, it has become possible to measure texture extremely rapidly with no sample rotation. In this paper, the details of the measurement and analysis methods are introduced.

## 2. Method

### 2.1. Instrument

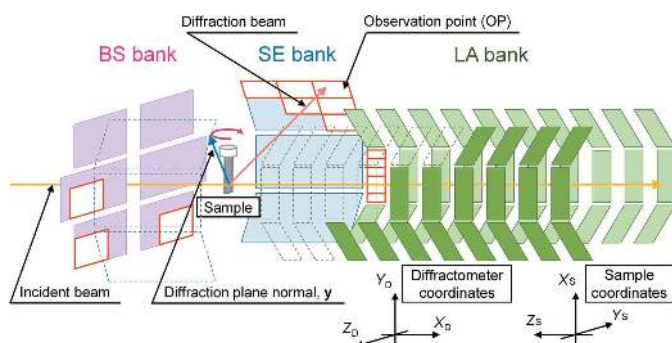
The TOF diffractometer iMATERIA (BL20 at MLF/J-PARC, Japan) has a vacuum sample chamber and multiple detector banks covering a wide  $2\theta$  range. Detailed specifications can be found in a previous paper (Ishigaki *et al.*, 2009).

Fig. 1 is a schematic diagram of the detector banks of iMATERIA. For texture measurements, the backscatter (BS,  $145 \leq 2\theta \leq 175^\circ$ ), special environment (SE,  $79 \leq 2\theta \leq 101^\circ$ ) and low-angle (LA,  $12 \leq 2\theta \leq 40^\circ$ ) detector banks are used. The banks are further separated into small regions called the ‘observation points’ (OPs). Each OP is assumed to behave as a point detector that measures the diffraction spectrum. The spectrum includes the Bragg diffraction peaks from various (*hkl*) crystallographic planes. Let  $\mathbf{y}'$  be the normal direction of the (*hkl*) plane in the diffractometer coordinate system,  $X_D$ – $Y_D$ – $Z_D$ .  $\mathbf{y}'$  can be calculated from the positional vector of the OP,  $\mathbf{p}$ , as

$$\mathbf{y}' = \mathbf{p}/|\mathbf{p}| - \mathbf{e}_{X_D}, \quad (1)$$

where  $\mathbf{e}_{X_D}$  is the unit vector along  $X_D$ , which is parallel to the incident beam. The sample loader of iMATERIA can rotate the sample around the  $Y_D$  axis on the measurement position. Therefore, the coordinate conversion matrix  $\mathbf{\Omega}(\omega)$ , a function of the rotation angle  $\omega$ , should be applied in order to obtain the (*hkl*) normal in sample coordinates,  $\mathbf{y}$ , as

$$\mathbf{y} = \mathbf{\Omega}\mathbf{y}'. \quad (2)$$



**Figure 1**  
Schematic diagram of texture measurement using the iMATERIA instrument.

The sizes of the OPs were determined such that the angular tolerance of  $\mathbf{y}$  was smaller than  $3^\circ$ .

### 2.2. Analysis

Conventional texture analysis is based on pole figure measurements. In this method, the diffraction intensities from several planes  $\{hkl\}$  are measured along  $\sim 1000$  different  $\mathbf{y}$  vectors (Kocks *et al.*, 1998). Rietveld texture analysis (Matthies *et al.*, 1997, 1999; Wenk *et al.*, 2010), which was applied in this study, uses diffraction spectra corresponding to various  $\mathbf{y}$  as the input for the ODF calculation. Fig. 2(a) shows some spectra used in the following analysis. Since the spectra include many diffraction peaks, the number of  $\mathbf{y}$  vectors required for quantitative analysis can be fewer than that for pole-figure-based ODF analysis. The diffraction intensities in the spectra are evaluated by Rietveld analysis or spectral fitting. At the first fitting, a uniform ODF corresponding to no texture is applied. Hence, the diffraction intensities of some peaks are overestimated while those of others are underestimated. The differences in the diffraction intensities between the measured and calculated spectra indicate the axis densities along  $\mathbf{y}$ . Therefore, the spectra can be regarded as ‘input inverse pole figures’, which contain the data points at the red dots in Figs. 2(b) and 2(c). ODFs are calculated based on them and the results are passed back to the Rietveld analysis, resulting in better fitting. By repeating the paired Rietveld refinements and the ODF calculation several times, both the spectral fitting and the ODF converge to the most likely solutions. More details on Rietveld texture analysis can be found in the literature by the developers (Matthies *et al.*, 1997; Wenk *et al.*, 2010).

In this study, the MAUD (materials analysis using diffraction) software package (Wenk *et al.*, 2010) was used to conduct the above analysis. This software has a ‘HIPPO wizard’ function to treat spectra measured at HIPPO, a TOF neutron diffractometer at the Los Alamos Neutron Science Center (LANSCE), USA (Wenk *et al.*, 2003). Because the structure of iMATERIA is somewhat similar to that of HIPPO, the HIPPO

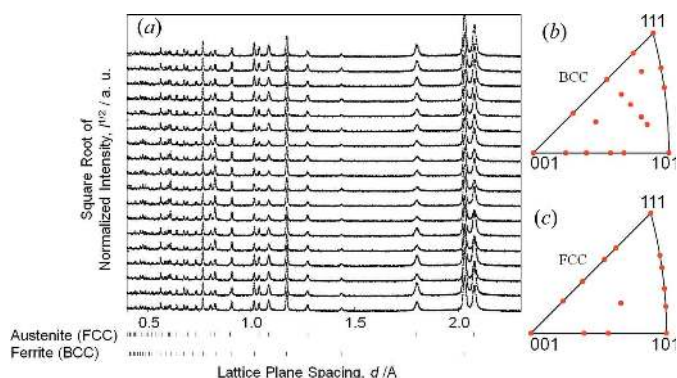


**Figure 2**  
(a) Diffraction spectra for the duplex stainless steel NAS64 after rolling to a thickness reduction of 20%. The spectra were acquired at the OPs at  $2\theta = 90^\circ$  of iMATERIA. (b) The distribution of the diffraction plane normal vectors seen in the spectra on the crystal coordinates for the ferrite phase and (c) that for the austenite phase.

**Table 1**  
Chemical composition of the NAS64 duplex stainless steel (mass%).

C	Si	Mn	Ni	Cr	Mo	W	N	Fe
0.01	0.4	0.7	6.5	25	3.3	0.1	0.17	Balance

wizard could be used to import the spectra acquired at iMATERIA. The unique instrumental parameters of iMATERIA were supplied by a separate instrumental parameter file. However, the incident beam profile used at iMATERIA was too complex for the preset incident beam profile functions to reproduce the profile shape. For this reason, the input spectra were externally normalized (Izumi *et al.*, 1987). The  $d$  range for the analysis was set so that each spectrum contained  $\sim 20$ – $30$  diffraction peaks for each phase. For steel samples with cubic crystal structures, a  $d$  range from 0.4 to 2.3 Å was used, as shown in Fig. 2(a). Since iMATERIA was designed as a powder diffractometer, the  $d$ -spacing resolution was high even for values below 1 Å. Therefore, iMATERIA could find many peaks with minimum overlapping ambiguity (Matthies *et al.*, 1997).

The entropy-modified Williams–Imhof–Matthies–Vinel (E-WIMV) method (Lutterotti *et al.*, 2004) was employed as the ODF calculation method. Although MAUD also provides the conventional harmonic expansion method, discrete ODF calculation methods such as E-WIMV are more suitable for strongly textured engineering samples, *e.g.* electrical steel (Matthies *et al.*, 2005).

Since we focused on texture analyses for metallic engineering materials, the resolution of the ODF (voxel size in Euler space) was set to  $5^\circ$ . This is the same resolution as that usually constructed by monochromatic X-ray measurements (Kocks *et al.*, 1998).

### 2.3. Samples

A rolled sheet of NAS64 duplex stainless steel (JIS SUS329J4L, ASTM A240) was supplied by the Nippon Yakin Kogyo Co. Ltd. The chemical composition is given in Table 1. The supplied sheet was additionally cold-rolled to a thickness reduction of 20% in the laboratory. The steel contained two phases,  $\sim 60$  mass% of body-centred cubic (b.c.c.) ferrite and  $\sim 40$  mass% of face-centred cubic (f.c.c.) austenite. Using Rietveld texture analysis, the textures in multiphase materials can be determined even with overlapping dominant peaks.

### 2.4. Measurement schemes

As stated in §2.2, Rietveld texture analysis uses diffraction spectra along various  $\mathbf{y}$  as the input. However, the number of spectra necessary to calculate a quantitative ODF with a resolution of  $5^\circ$  was unclear. In order to determine the optimal number of spectra, we firstly set 36 OPs. Therefore, 36 spectra were obtained by one exposure of the neutron beam without sample rotation. A stereographic projection of the distribution of  $\mathbf{y}$  is shown in Fig. 3(a). By repeating this measurement at different sample angles  $\omega$  (rotation around  $Y_D$ ), the total

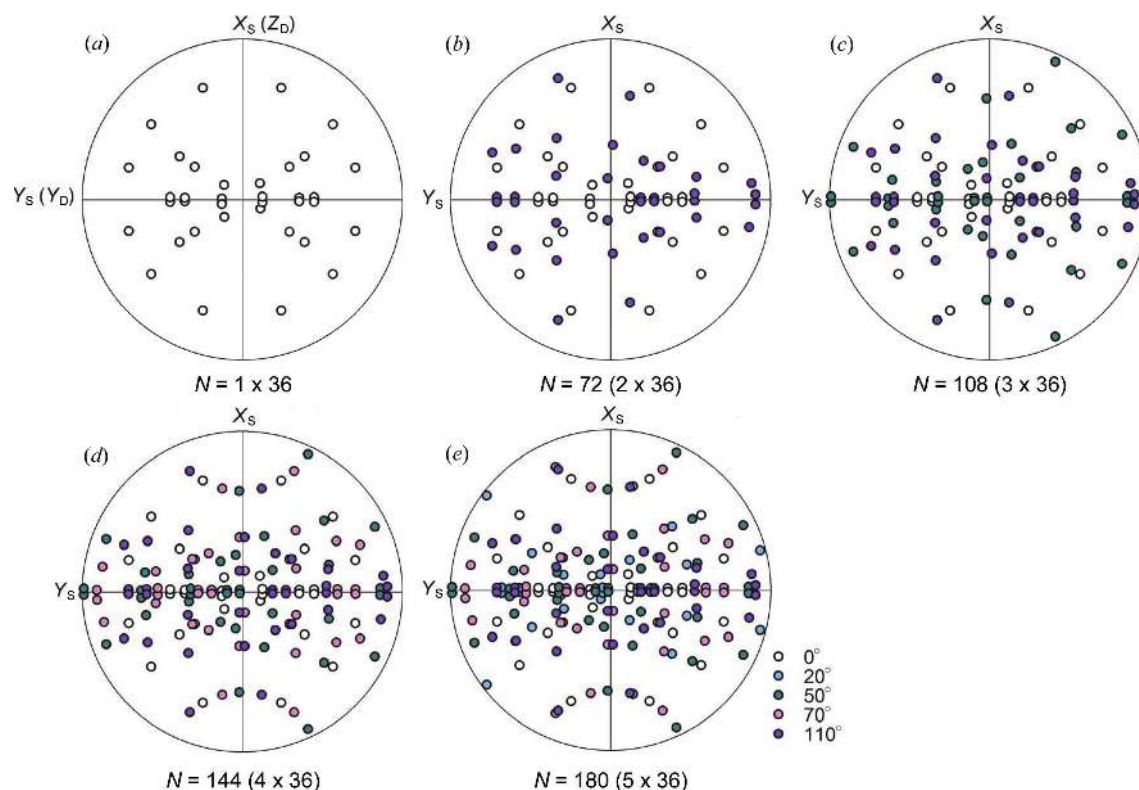


**Figure 3**  
(a) The distribution of the pole directions  $\mathbf{y}$  corresponding to the spectra measured by the 36 OPs. (b)–(e) Distributions of  $\mathbf{y}$  resulting from multiple exposures at different  $\omega$  angles.  $N$  indicates the total number of spectra used in the calculation.

number of spectra ( $N$ ) can be multiplied. Figs. 3(b)–3(e) depict the distribution of  $\mathbf{y}$  in the sample coordinate system achieved by multiple measurements. In this way,  $N$  can be increased indefinitely, while the total measurement time is also increased. Additionally, calculations using *MAUD* become very time consuming when hundreds of spectra are provided.

In order to realize fast measurement and analysis, an alternative measurement scheme is suggested using the 132 OPs shown in Fig. 4. In this case, the 132 spectra can be obtained simultaneously without sample rotation. This enables rapid texture measurement, requiring only 1–3 min of data acquisition without sample rotation. Hereinafter, the results from the above schemes are referred to by  $N$ , where  $N = n \times 36$  ( $n = 1, 2, \dots, 5$ ) indicates results from the former scheme and  $N = 132$  corresponds to the latter.

The measurements were conducted at a beam power of 500 kW. The receiving frequency for the incident pulse neutron was 25 Hz.

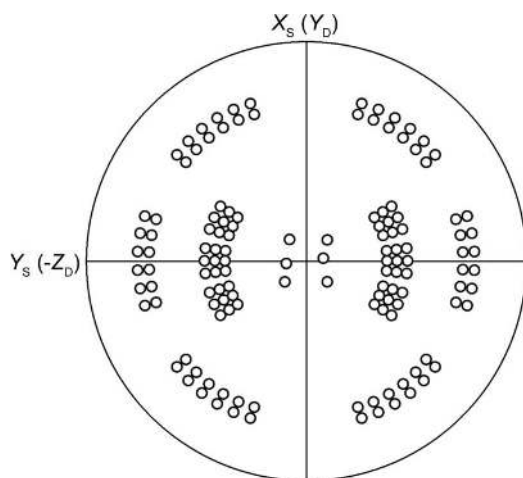


**Figure 4**  
The distribution of 132 OPs in sample (diffractometer) coordinates for the rapid measurement scheme.

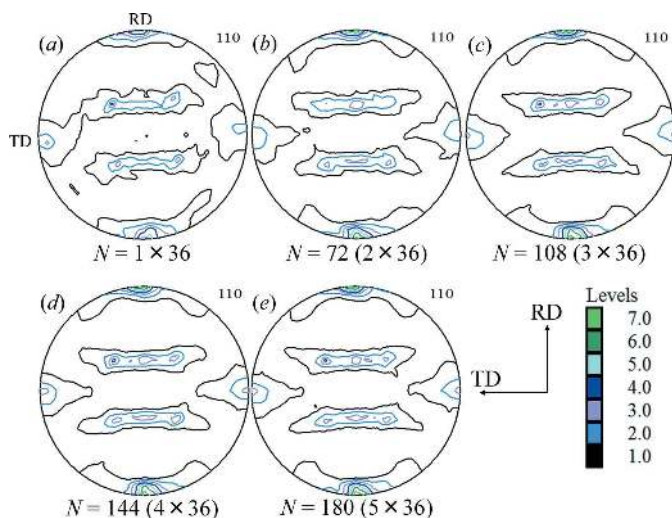


**Figure 5**  
{110} pole figures of the ferrite phase in the 20% rolled duplex stainless steel obtained by analyses with different numbers of input spectra,  $N$ .

### 3. Results and discussion

#### 3.1. Optimal number of spectra for texture analysis

Figs. 5 and 6 show the {110} pole figures for the ferrite and austenite phases in the 20% rolled duplex stainless steel analysed with different numbers  $N$  of input spectra. All show the well known conventional pole distributions for rolled textures (Hamada *et al.*, 2003; Hirsch & Lücke, 1988). However, the maximum intensity is somewhat low for cases where  $N < 108$ . The contour lines are rough with insufficient  $N$ , implying a lack of input data to construct the ODF. With  $N \geq 108$ , these problems are suppressed and the features of the pole figures are not affected by  $N$ . Hence, it can be said that the quality of the pole figure is saturated for  $N > 100$ .

#### 3.2. Rapid measurement scheme

From the above discussion, the number of spectra  $N$  for texture analysis must exceed 100. This indicates that the rapid measurement scheme using 132 OPs (Fig. 4) can also provide a quantitative texture analysis.

Fig. 7 shows the calculated pole figures for the ferrite and austenite phases using the rapid measurement scheme,  $N = 132$ . The figures agree well with the results shown in Figs. 5 and 6. It seems that the homogeneity of the distribution of OPs is not as important as the number of OPs, by considering the differences between Figs. 3 and 4.

For a more detailed texture analysis, metallurgists often examine textures using the ODF in Euler space rather than pole figures. The ODFs in Bunge's Euler space ( $\varphi_1, \Phi, \varphi_2$ ) were constructed from the pole figures exported by *MAUD* using the *LaboTex* software (Pawlik & Ozga, 1999). Because six complete pole figures were used as input for calculating the ODF for each phase, the ambiguity introduced in this process is negligible. In the reconstruction, orthorhombic sample symmetry was applied, resulting in  $\varphi_1$  values ranging between 0 and 90°.

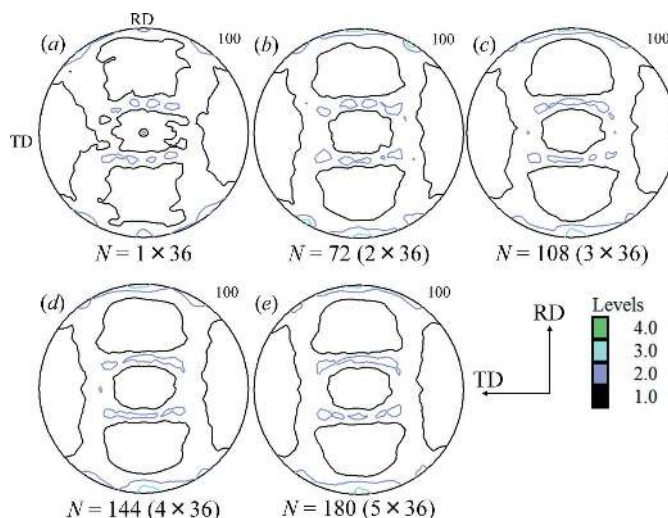


**Figure 6**  
{100} pole figures of the austenite phase in the 20% rolled duplex stainless steel obtained by analyses with different numbers of input spectra,  $N$ .

**Table 2**

Volume fraction of texture components in the ferrite phase of the 20% rolled duplex stainless steel (%).

	{001}<110>	{112}<110>	{111}<110>	{111}<112>
$N = 1 \times 36$	12.6	5.7	2.8	2.9
$N = 2 \times 36$	13.2	8.2	4.0	5.0
$N = 3 \times 36$	13.6	7.5	3.9	5.2
$N = 4 \times 36$	14.3	8.1	4.2	5.5
$N = 5 \times 36$	13.7	8.0	4.2	5.6
$N = 132$	14.3	7.3	3.3	4.7

The  $\varphi_2 = 45^\circ$  cross sections of the ODFs for both the ferrite and austenite phases are shown in Fig. 8. The results of the scheme used in the previous section ( $N = 5 \times 36$  OP) are also indicated. The results of the rapid scheme with  $N = 132$  (Figs. 8*b* and 8*d*) show good agreement with those from the  $N = 5 \times 36$  scheme. In addition, both phases indicate familiar rolled textures. The texture of the ferrite phase consists of  $\alpha$  ( $\{h\bar{h}l\}$ <110>) and  $\gamma$  ( $\{111\}$ < $uvw$ >) fibres (Hamada *et al.*, 2003), while that of the austenite phase has brass ( $\{110\}$ <112>), Goss ( $\{110\}$ <001>) and copper ( $\{112\}$ <111>) components (Hirsch & Lücke, 1988).

In order to verify that quantitative texture component analysis is possible using the new method, the volume fractions of some common texture components were calculated. The volume fraction  $V(g)$  of a texture component at an orientation  $g(\varphi_1, \Phi, \varphi_2)$  can be calculated as

$$\begin{aligned}
 V(g) &= \frac{1}{8\pi^2} \int_{\Delta g} f(g) dg \\
 &= \frac{1}{8\pi^2} \int_{\varphi_2 - \Delta\varphi_2}^{\varphi_2 + \Delta\varphi_2} \int_{\Phi - \Delta\Phi}^{\Phi + \Delta\Phi} \int_{\varphi_1 - \Delta\varphi_1}^{\varphi_1 + \Delta\varphi_1} f(\varphi_1, \Phi, \varphi_2) \sin \Phi d\varphi_1 d\Phi d\varphi_2.
 \end{aligned}
 \tag{3}$$

In this study, the tolerance angles  $\Delta\varphi_1 = \Delta\Phi = \Delta\varphi_2 = 10^\circ$  were applied. The results are listed in Tables 2 and 3 for the ferrite and austenite phases, respectively. It is seen that the volume fractions of the texture components are almost constant above  $N = 72$  ( $= 2 \times 36$ ). The differences fall within 0.8%. Further-

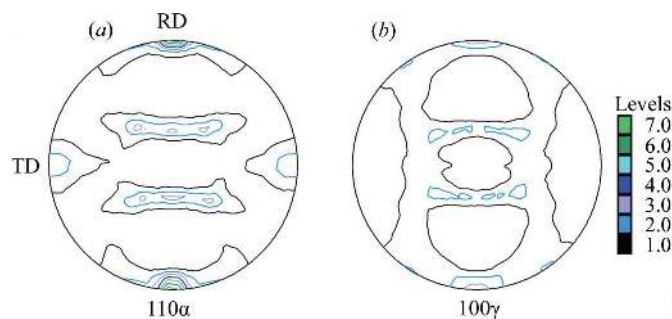


**Figure 7**  
(a) The {110} pole figure of the ferrite phase and (b) the {100} pole figure of the austenite phase for the 20% rolled duplex stainless steel, calculated by the optimized method using 132 OPs.

**Table 3**

Volume fraction of texture components in the austenite phase of the 20% rolled duplex stainless steel (%).

	{110}<112>	{110}<001>	{112}<111>	{132}<643>
$N = 1 \times 36$	9.1	3.6	5.0	11.5
$N = 2 \times 36$	10.6	5.0	6.5	14.7
$N = 3 \times 36$	10.3	5.5	6.6	14.5
$N = 4 \times 36$	10.6	5.7	7.1	14.7
$N = 5 \times 36$	11.0	5.5	7.1	15.0
$N = 132$	10.9	5.4	6.1	14.5

**Table 4**

Mass fraction of austenite phase in the 20% rolled duplex stainless steel.

$N$	1 × 36	2 × 36	3 × 36	4 × 36	5 × 36	132
Mass fraction (%)	40.9	43.7	45.5	45.5	44.1	43.5

more, the orders of volume fractions in both phases are also constant above  $N = 72$ , including  $N = 132$ .

Table 4 shows the analysed weight fractions of the austenite phase with different  $N$ . Again, the values obtained with  $N \geq 72$  are similar, whereas the phase fraction with  $N = 36$  is a little smaller than the others. Since the phase fraction is determined from the diffraction intensities, the correct values can be obtained when accurate texture analyses are conducted for both phases. Therefore, these results also imply convergence of the Rietveld texture analysis with the data from iMATERIA with  $N \geq 72$ .

Thus, the TOF neutron diffractometer iMATERIA is capable of detailed texture measurement with ODF analysis, which is often conducted on the basis of the results of conventional X-ray texture measurements. The most striking feature of the present method is the very short time required for the measurement. The complete ODF for steel can be

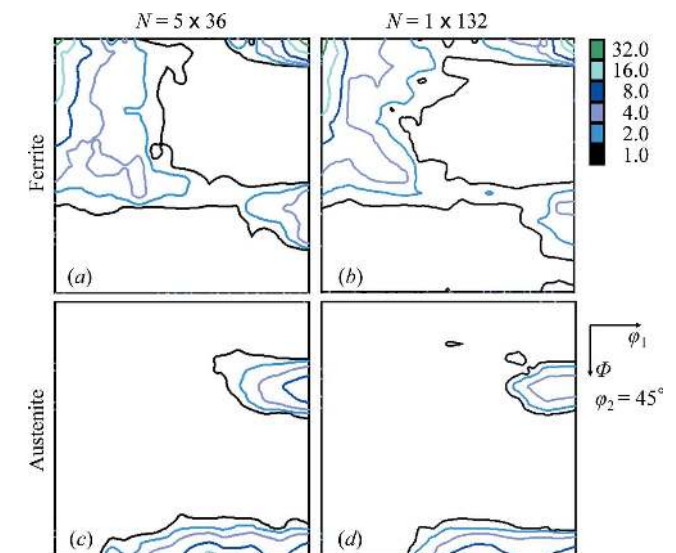


**Figure 8**  
 $\varphi_2 = 45^\circ$  sections of the ODFs for the ferrite phase in the 20% rolled duplex stainless steel calculated with (a)  $N = 180$  ( $5 \times 36$  OPs) and (b)  $N = 132$ , and for the austenite phase calculated with (c)  $N = 180$  ( $5 \times 36$  OPs) and (d)  $N = 132$ .

obtained within a few minutes of exposure. This is especially beneficial for the *in situ* measurement of textures during deformation and annealing. The authors are now developing suitable deformation and heating environments for such *in situ* measurements.

### 4. Conclusions

A texture measurement system using Rietveld texture analysis has been developed using iMATERIA, a TOF neutron diffractometer at MLF/J-PARC, Japan. By optimizing the analysis method, a very fast texture measurement system has been developed. The main results of this study are as follows.

(1) Rapid quantitative texture analysis is possible within a few minutes for duplex stainless steels using iMATERIA, which is equipped with numerous detectors covering a wide range of scattering angle and has a high *d*-spacing resolution at a beam power of 500 kW.

(2) Rietveld analysis has been employed to analyse the texture of the material by deducing the ODF from many TOF diffraction spectra having a high *d*-spacing resolution.

(3) The number of diffraction spectra required for a reliable and quantitative texture analysis was determined experimentally at about 100. The rapid texture measurement scheme thus developed consists of 132 spectra acquired in a few minutes without any rotation of the sample.

### Acknowledgements

The authors would like to express their appreciation to Dr S. Vogel for instructive discussions on the basic concept of Rietveld texture analysis. We thank Dr H. Inoue for his

helpful comments and suggestions. We are also grateful to Dr Minemura and Dr Tomida for their kind and constant support.

### References

- Hamada, J., Matsumoto, Y., Fudanoki, F. & Maeda, S. (2003). *ISIJ Int.* **43**, 1989–1998.
- Hirsch, J. & Lücke, K. (1988). *Acta Metall.* **36**, 2863–2882.
- Ishigaki, T. *et al.* (2009). *Nucl. Instrum. Methods Phys. Res. Sect. A*, **600**, 189–191.
- Izumi, F., Asano, H., Murata, H. & Watanabe, N. (1987). *J. Appl. Cryst.* **20**, 411–418.
- Juul Jensen, D. & Kjems, J. K. (1983). *Texture Microstruct.* **5**, 239–251.
- Kocks, U. F., Tomé, C. N. & Wenk, H. R. (1998). *Texture and Anisotropy*, pp. 102–149. Cambridge University Press.
- Lutterotti, L., Chateigner, D., Ferrari, S. & Ricote, J. (2004). *Thin Solid Films*, **450**, 34–41.
- Matthies, S., Lutterotti, L., Ullemeyer, K. & Wenk, H. R. (1999). *Texture Microstruct.* **33**, 139–149.
- Matthies, S., Lutterotti, L. & Wenk, H. R. (1997). *J. Appl. Cryst.* **30**, 31–42.
- Matthies, S., Pehl, J., Wenk, H.-R., Lutterotti, L. & Vogel, S. C. (2005). *J. Appl. Cryst.* **38**, 462–475.
- Oles, A., Kulka, J., Szpunar, J. & Wawszczak, R. (1985). *Neutron Scattering in the Nineties*, 14–18 January 1985, Jülich, Germany. *IAEA Proceedings Series*, pp. 533–538. Vienna: International Atomic Energy Agency.
- Onuki, Y., Hongo, R., Okayasu, K. & Fukutomi, H. (2013). *Acta Mater.* **61**, 1294–1302.
- Pawlik, K. & Ozga, P. (1999). *Göttinger Arb. Geol. Paläontol.* SB4.
- Truszkowski, W., Krol, J. & Major, B. (1982). *Metall. Trans. A*, **13**, 665–669.
- Wenk, H.-R. (1991). *J. Appl. Cryst.* **24**, 920–927.
- Wenk, H., Lutterotti, L. & Vogel, S. (2003). *Nucl. Instrum. Methods Phys. Res. Sect. A*, **515**, 575–588.
- Wenk, H., Lutterotti, L. & Vogel, S. C. (2010). *Powder Diffr.* **25**, 283–296.